Cancellation of probe effects in measurements of spin-polarized momentum density by electron–positron annihilation

2006 J. Phys.: Condens. Matter 18 L289

(http://iopscience.iop.org/0953-8984/18/22/L03)

INSTITUTE OF PHYSICS PUBLISHING JOURNAL OF PHYSICS: CONDENSED MATTER

J. Phys.: Condens. Matter **18** (2006) L289–L295 doi:10.1088/0953-8984/18/22/L03

LETTER TO THE EDITOR

Cancellation of probe effects in measurements of spin-polarized momentum density by electron–positron annihilation

M Biasini[1,3] **and J Rusz**[2]

[1] Department of Physics, University of California at Riverside, Riverside, CA 92521, USA
[2] Department of Electronic Structures, Charles University, Ke Karlovu 5, 12116 Prague 2, Czech Republic

Received 5 February 2006
Published 16 May 2006
Online at stacks.iop.org/JPhysCM/18/L289

Abstract

Measurements of the two-dimensional angular correlation of the electron–positron annihilation radiation have been done in the past to detect the momentum spin density and the Fermi surface. We point out that the momentum spin density and the Fermi surface of ferromagnetic metals can be revealed in great detail owing to the large cancellation of the electron–positron matrix elements which in paramagnetic multiatomic systems plague the interpretation of the experiments. We prove our conjecture by calculating the momentum spin density and the Fermi surface of the half metal CrO_2, which has received large attention due to its possible applications as a spintronics material.

(Some figures in this article are in colour only in the electronic version)

To a great extent, the Fermi surface (FS) can be regarded as the defining property of a metal. It is an ubiquitous concept which appears in numberless works devoted to the study of the electronic structure of systems which, under some particular circumstance, seem to show metallic behaviour. In several cases, the initial task of establishing metallic behaviour is not easy since different probes can yield contrasting answers. Clearly, an experimental investigation of the FS implies the observability of the electrons sitting in the *partially filled* energy bands, which, in turn, requires interaction of the conduction electrons with the experimental probe.

In the case of a measurement of the two-dimensional angular correlation of electron–positron annihilation radiation (2D-ACAR), the FS is revealed through discontinuities (breaks) in the electron–positron momentum density, $\rho^{\mathrm{ep}}(\mathbf{p})$ [1], at points $\mathbf{p}_{\mathrm{F}} = (\mathbf{k}_{\mathrm{F}} + \mathbf{G})$, where $\mathbf{G}$ is a reciprocal lattice vector and $\mathbf{k}_{\mathrm{F}}$ are the reduced Fermi wavevectors in the first Brillouin zone (BZ). While the locations of the FS breaks are faithfully preserved [2], the resulting single

[3] ENEA, via don Fiammelli 2, 40129 Bologna, Italy.

particle electron momentum density, $\rho^e(\mathbf{p})$, is severely modulated by the non-uniform positron (spatial) density and the electron–positron Coulomb interaction. In this letter we show that, in the special case of a ferromagnetic sample, the probe modulation is strongly suppressed, allowing a faithful representation of the spin-polarized momentum density and unambiguous interpretation of the data. The FS breaks are reinforced by the Lock–Crisp–West (LCW) transformation [3], consisting of folding the momentum distribution $\rho^{\mathrm{ep}}(\mathbf{p})$ back onto the first BZ by translation over the appropriate vectors $\mathbf{G}$. The result of the summation (denoted as LCW density) is [4]

$$\rho^{\mathrm{ep}}_{\mathrm{LCW}}(\mathbf{k}) = \sum_n \theta(E_{\mathrm{F}} - \epsilon_{\mathbf{k},n}) \int |\psi^n_{\mathbf{k}}(\mathbf{r})|^2 |\phi(\mathbf{r})|^2 g(\mathbf{r})\, \mathrm{d}\mathbf{r}. \tag{1}$$

Here $\psi^n_{\mathbf{k}}$ and ϕ denote the electron and positron wavefunction, respectively, E_{F} is the Fermi level and $\epsilon_{\mathbf{k},n}$ is the energy eigenvalue of the electron from band n with Bloch wavevector $\mathbf{k}$. The enhancement factor [5], $g(\mathbf{r})$, describes the enhancement of the electronic density at the positron location due to the Coulomb force. If the $\mathbf{k}$, n dependence of the overlap integral in equation (1) is negligible, $\rho^{\mathrm{ep}}_{\mathrm{LCW}}(\mathbf{k})$ is reduced to the *occupancy*, i.e. the number of occupied bands per $\mathbf{k}$-point. The FS manifolds are the loci of the breaks of the occupancy. A significant drawback of 2D-ACAR is that all the outer electrons overlap (to some extent) with the positron probe. Therefore, when the orbital character of one full valence band changes noticeably in the BZ, the related LCW density acquires a $\mathbf{k}$-dependence which is superimposed to the changes in the occupancy due to the FS breaks of the conduction bands. For example, our recent work on UGa_3 [6] has detected a noticeable change in the p character of three valence bands located 1–2 eV below E_{F} which greatly obscured the visibility of the FS. Further notable examples are high-T_{c} superconductors, where strong positron wavefunction effects prevented the observation of the critical FS sheets linked to the copper oxide planes, which are responsible for superconductivity [7, 8].

Obviously, the elimination of the contribution of all the filled bands from the LCW summation would greatly increase the visibility of the FS whenever the overlap integral of equation (1) is $\mathbf{k}$(valence)-dependent. This favourable situation is indeed realized in the measurement of the spin-polarized bands of ferromagnetic metals. In this case, the employment of 2D-ACAR experiments [9–13] hinges on two facts: (i) the intrinsic polarization P_{e^+} for positrons produced during β-decay (for the ^{22}Na source P_{e^+}, averaged over angle and velocity, is about 36%); (ii) the annihilation selection rule, which requires that the positron may undergo 2γ annihilation only if the spins of the annihilating pair form a singlet state.

Therefore, two 2D-ACAR measurements performed when the magnetic substance is polarized (by an external magnetic field) in directions respectively parallel and antiparallel to the average positron polarization (which is unchanged upon reversal of the magnetic field) will detect an imbalance of 2γ annihilations with respect to the majority or minority spins.

The experimental spectra taken when the positron polarization is parallel (antiparallel) to the polarizing magnetic field are then

$$\rho^{\mathrm{ep}}_{\mathrm{par,antipar}}(\mathbf{p}) = 1/2(1 \pm P_{\mathrm{e}^+})[N^{\mathrm{M}}(\mathbf{p}) + N^{\mathrm{NM}}(\mathbf{p})/2] + 1/2(1 \mp P_{\mathrm{e}^+})[N^{\mathrm{m}}(\mathbf{p}) + N^{\mathrm{NM}}(\mathbf{p})/2]. \tag{2}$$

Here, N^{M} and N^{m} denote the momentum density of majority and minority spins bands, which contribute to the net magnetization. Furthermore, in equation (2) we have separated a contribution, denoted as N^{NM}, of all the other full bands which, even if they are spin split by exchange interaction, do not contribute either to the net magnetization or to the electron polarization at the Fermi surface (note that most often the exchange splitting for those bands is very small; see [14, 15] for the case of CrO_2). We therefore refer to N^{NM} as to the *non-magnetic* part of the electron momentum density.

Subtraction of $\rho^{\rm ep}_{\rm par}$ from $\rho^{\rm ep}_{\rm antipar}$ yields the net momentum spin density $\rho^{\rm ep}_{\rm spin}(\mathbf{p})$.

$$\rho^{\rm ep}_{\rm spin}(\mathbf{p}) = P_{\rm e^+}[N^{\rm M}(\mathbf{p}) - N^{\rm m}(\mathbf{p})]. \tag{3}$$

Equations (2) and (3) are equally applicable to the electron–positron momentum density, $\rho^{\rm ep}(\mathbf{p})$, or to the LCW density, yielding for the latter case, the LCW net spin density $\rho^{\rm ep}_{\rm LCW\ spin}(\mathbf{k})$.

Note that, whereas the subtraction present in equation (3) leads to the net momentum (or LCW) spin density, which after integration yields the total spin magnetic moment, the difference between *normalized* experimental spectra $\rho^{\rm ep-expt}_{\rm par}$, $\rho^{\rm ep-expt}_{\rm antipar}$ yields zero total spin moment by construction. Different remedies of this problem have been proposed [9–13], all hinged on some small renormalization of the experimental data prior to taking the difference $\rho^{\rm ep-expt}_{\rm par} - \rho^{\rm ep-expt}_{\rm antipar}$. Obviously, the FS related discontinuities are not shifted by any renormalization of the spectra.

The main point of this work is the disappearance of $N^{\rm NM}$ and all the positron wavefunction effects related to the bands in question. As obvious as it may appear, this interesting result has, to our knowledge, never been pointed out and should prove to be very useful in future studies of ferromagnetic metals.

To investigate our conjecture we have chosen to examine CrO_2, which is predicted to be a half metal by a variety of *ab initio* band structure calculations [16, 14, 17, 18]. Due to this result CrO_2 has attracted much attention in the field of spintronics for its potential use as injector of a highly (nominally 100%) spin-polarized current in the future *field effect spin transistor*. A puzzling result of the calculations is that different recipes to approximate the exchange correlation potential, $U_{\rm xc}$ (local spin density approximation (LSDA) [19] and generalized gradient approximation (GGA) [20]), lead to unusually noticeable differences in the FS topology [14]. A further interesting result is that the standard LSDA and GGA seem to explain ultraviolet photoemission spectroscopy (UPES) experiments [21] better than the LDA + U method, [18], which usually is more suited to treating strong electron correlations.

In [6, 15] we have presented a method to calculate directly the LCW density via equation (1). As a base for our calculation we used the scalar relativistic full-potential linearized augmented plane waves method (FP-LAPW) implemented in the WIEN2k package [22]. Compared to similar works of other authors [23, 4], our scheme, including electron–positron correlation effects [5], being *full potential* and compatible with any option of WIEN2k, which include spin–orbit (so) interaction, LDA + U and orbital polarization, is more suited to the study of narrow bands and electron correlations.

The extension of the scheme to spin-polarized calculations is relatively straightforward. The same steps used in the paramagnetic calculations are done for spin-up and spin-down electrons separately. In the absence of so interaction the result consists of *pure* up-spin and down-spin bands. After the inclusion of so, each Bloch state becomes a combination of spin-up and spin-down components. For each band crossing $E_{\rm F}$ there is now an up-spin and down-spin submanifold, both having the same occupancy (and therefore the same Fermi surface). The amplitudes of these submanifolds are, however, different. Owing to parity and angular momentum conservation, the positron essentially *projects* the electronic states over the spin-up or spin-down manifolds.

The crystal structure of CrO_2 is simple tetragonal (rutile type, space group $P4_2/mnm$, [16]) with two formula units per unit cell. Details of the calculations, performed adopting $U_{\rm xc}$ according to GGA and LDA in the paramagnetic and ferromagnetic phases, are reported elsewhere [24]. The calculated majority spin bands are in excellent agreement with those reported by Mazin *et al* [14]. The main finding of the calculation is the half metallic behaviour, with a large energy gap ($\simeq$2 eV) in the minority spin bands. The conduction bands

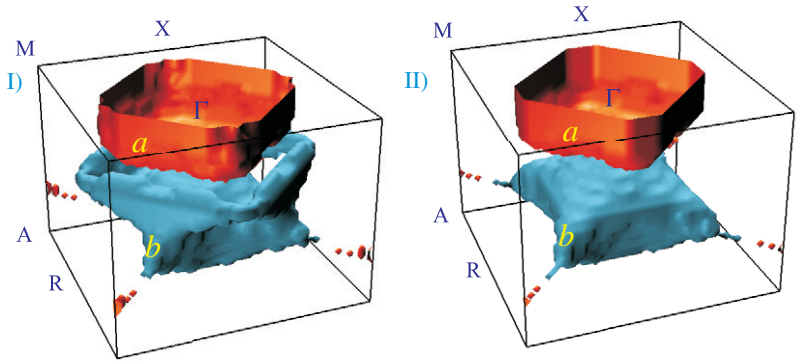

Figure 1. The two FS sheets (*a*, *b*) of FM CrO_2, shown in half the BZ (*a* orange, electronlike; *b* blue, holelike) produced with U_{xc} from LSDA (I) and GGA (II) [19, 20]. Here and in the next figures capital letters label the high symmetry points of the BZ.

have a very strong Cr d character, which is ascribed to states of t_{2g} symmetry. It is worth noting that the Cr d orbital character of all the conduction bands is rather constant along each of the high symmetry directions.

As mentioned above, the topology of the holelike FS sheet, shown in figure 1((I, II)b) depends noticeably on the kind of U_{xc} (LSDA, GGA). Whereas in the GGA case this FS has a simple, pillow-like shape (figure 1(II-b)), the corresponding FS manifold resulting from LSDA (figure 1(I-b)) is a pseudosphere connected to a toroidal structure with rhombic shape. On the other hand, the electronlike, Γ-centred structure, yielded by the two calculations is very similar. Since CrO_2 is a compensated metal (a necessary condition of any half metal), the electronlike and holelike sheets have equal volume. The Fermi volumes resulting from LSDA and GGA differ slightly, corresponding to 12.8% of the BZ and 10.7% of the BZ for LSDA and GGA, respectively.

The predicted response of a 2D-ACAR experiment can be elucidated by a slice of the calculated LCW density (adopting LSDA) in the (010) plane (GGA yields little difference in this plane; recall figure 1). In figure 2 panels (a) and (b) refer to the majority and minority spins LCW densities, respectively, whereas panels (c) and (d) denote the sum and difference of panels (a) and (b). These panels would be obtained by an experiment with 100% spin-polarized positrons impinging a sample where the polarizing magnetic field is parallel or antiparallel to the positron polarization. In panel (a) the breaks pertaining to the electronlike and holelike FS sheets appear rather clearly (compare the changes of grey scale (or colour) with the contour line marking the FS breaks), in spite of a strong modulation caused by a non-uniform positron density. This modulation is the only feature appearing in panel (b), consistent with a negligible spin up–down mixing due to so (WIEN2k yields 99.97% electron polarization at E_F). In panel (c) we have summed panels (a) and (b) and noticed that positron wavefunction effects are reinforced at the expense of the FS signatures.

The very appealing message, and the main point of this letter, is however provided by panel (d), where most of the positron wavefunction effects cancel out and the almost intact topology of the FS is restored.

This result proves our conjecture that the LCW densities of the up–down full and weakly spin polarized bands, denoted by an overall $N^{NM}(\mathbf{k})$, differ negligibly. Therefore, the difference up–down essentially eliminates the contribution from those bands and any positron wavefunction effect to be ascribed to them. The cancellation of positron effects caused by all the *non-magnetic bands* is clearly of great importance in systems with several atoms in the

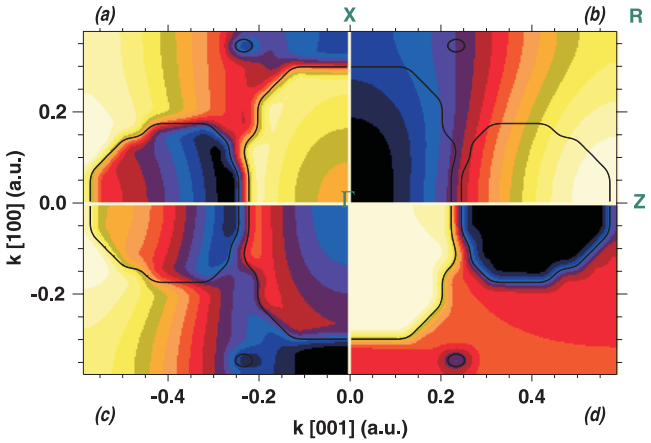

Figure 2. FLAPW calculations for CrO_2 in the (010) plane of the tetragonal BZ: (a) up-spin LCW density; (b) down-spin LCW density; (c) (a) + (b); (d) (a) − (b). The black contour denote the intersections of the two main FS sheets (see figure 1) with the (010) plane. Note that the horizontal direction is along [001].

unit cell and, consequently, several bands near to E_F. A similar effect can be inferred from figure 9 of [11], referring to the half metal NiMnSb. In CrO_2 the visibility of the FS is further enhanced by the weakness of the positron modulation of the conduction bands. This result is consistent with the constancy of the d orbital character in the BZ for all the conduction bands, noted above.

The similarity of panel 2(d) with the theoretical occupancy (whose breaks denote the FS) makes feasible algorithms aimed at extracting the FS from isodensity surfaces of the LCW density. This task would be impossible for the data set shown in panel 2(a), where, owing to positron modulation, the amplitude of the LCW density along the Fermi break of a single sheet changes noticeably in the BZ. Conversely, $\rho^{ep}_{LCW\ spin}(\mathbf{k})$ presented in panel 2(d) allows one to separate very clearly the two conduction bands and apply the method presented in [25] which identifies a multi-sheet FS in terms of isodensity surfaces selected at the loci of maximal amplitude variation of the LCW density. It is worth noticing that in the half metals the analysis of $\rho^{ep}_{LCW\ spin}(\mathbf{k})$ for the search of the FS manifolds is particularly suited. In fact, since the subtraction of the *insulating* LCW (down) spin density from the *conducting* LCW (up) spin density preserves the proper sign in the jumps of the occupancy due to the FS breaks, maxima of $\rho^{ep}_{LCW\ spin}(\mathbf{k})$ will correspond to maxima of the occupancy and vice versa. Figure 3 shows the resulting isodensity surfaces of $\rho^{ep}_{LCW\ spin}(\mathbf{k})$. The similarity with the true FS shown in figure 1 is striking. The cancellation of positron wavefunction effects shows that 2D-ACAR has the power to investigate the FS predictions of LSDA and GGA, shown in figure 1. The difference in the FS is well revealed in the (110) plane. To establish to what extent feasible experiments can accomplish this task, in figure 4 we have simulated in full the output of the experiment, according to equation (2). The steps adopted to produce figure 4 are, in succession: (i) calculation (adopting U_{xc} from GGA and LSDA) of $\rho^{ep}_{LCW\ par}(\mathbf{k})$ and $\rho^{ep}_{LCW\ antipar}(\mathbf{k})$ according to the mixing shown in equation (2), employing the realistic positron polarization $P_{e^+} = 0.35$; (ii) convolution of $\rho^{ep}_{LCW\ par}(\mathbf{k})$ and $\rho^{ep}_{LCW\ antipar}(\mathbf{k})$ with the experimental resolution R[4]; (iii) perturbation of the two simulated densities with statistical

[4] The adopted value $R = 0.0685$ a.u., corresponding to 9% of the BZ along the [100] direction, is typical of existing 2D-ACAR setups.

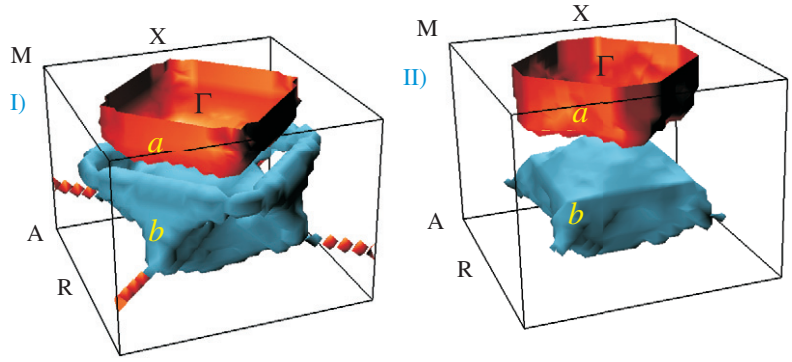

Figure 3. Spin-polarized FSs seen by 2D-ACAR experiments in CrO_2, shown in half the BZ (theoretical prediction). The FSs are identified by the two isodensity surfaces (*a*, *b*) extracted from $\rho^{ep}_{LCW\ spin}(\mathbf{k})$ as described in the text. (*a* orange, electronlike; *b* blue, holelike.) The pertaining LCW densities were produced with U_{xc} from LSDA (left, (I)) and GGA (right, (II)) [19, 20].

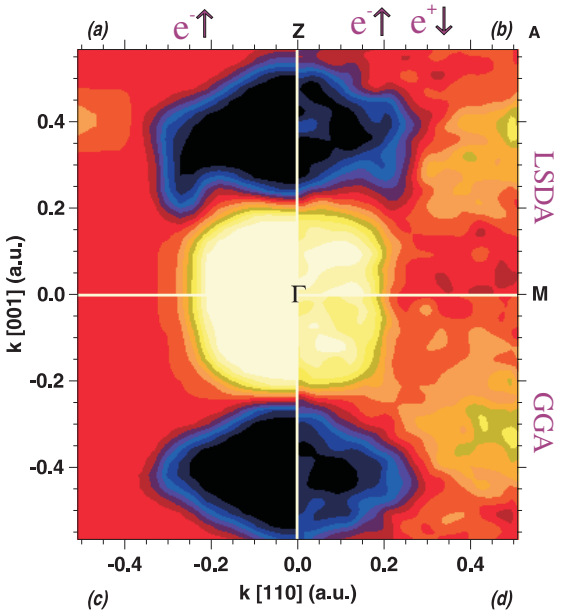

Figure 4. FLAPW calculations for CrO_2 in the (110) plane of the tetragonal BZ. (a) LSDA up-spin occupancy convoluted with the experimental resolution; (b) LSDA simulated experimental difference spectra (inclusive of statistical noise; see text), $\rho^{ep}_{LCW\ spin}(\mathbf{k})$; (c) same as (a) for GGA; (d) same as (b) for GGA.

noise. It is assumed that the LCW density was reconstructed from five projections, each collecting 5×10^8 coincidence counts, and that the spectra were symmetrized in the 3D reconstruction procedure [25]; (iv) construction of $\rho^{ep}_{LCW\ spin}(\mathbf{k})$.

Figure 4 shows the electronic occupancy (reflecting the FS topology) convoluted with the experimental resolution (panels (a), (c)] compared to the difference spectra resulting from steps (i)–(iv) (panels (b), (d)) for LSDA and GGA, respectively. Interestingly, the bulging of the

LSDA holelike FS at $\simeq(0.27, 0.20)$ a.u. (panel (a)), absent in the GGA holelike FS (panel (c)), is well reproduced by the difference $\rho^{\mathrm{ep}}_{\mathrm{LCW\,spin}}(\mathbf{k})$ (panel (b)) and not present in panel (d). Obviously, to reveal the FS subtleties at stake, arrays with large number of counts are required, particularly when differences between experimental spectra are analysed. With this caveat, we predict that a 2D-ACAR experiment should decide over this issue.

In conclusion, we have pointed out the power of the magnetic LCW procedure to eliminate a large part of the modulation of the LCW density due to the non-uniform positron density and reveal the FS in great detail. We have proved that this indeed happens by applying our scheme to calculate the LCW density of the half metal CrO_2. We have simulated in full the output of an experiment performed with partial polarization of the positron, dictating the amount of data collection required to have appropriate signal to noise ratios. Note that the ability to include the so effect can be employed to corroborate 2D-ACAR measurements aimed at determining the polarization of the conduction electrons at the Fermi surface. This type of information could be of critical importance for the design of novel materials to be employed in the implementation of the future spin-based FET.

We thank Allen Mills for stimulating discussions. This work was supported by DOD/DMEA—Agency No DMEA 94003-05-2-0504 and project MSM 0021620834 financed by Ministry of Education of Czech Republic.

References

[1] Berko S 1983 *Proc. Int. School Phys. Enrico Fermi* ed W Brandt and A Dupasquier (Amsterdam: North-Holland) p 64
[2] Majumdar C K 1965 *Phys. Rev.* **140** A227
[3] Lock D G, Crisp V H and West R N 1973 *J. Phys. F: Met. Phys.* **3** 561
[4] Kaiser J H, West R N and Shiotani N 1986 *J. Phys. F: Met. Phys.* **16** 1307
[5] Boronski E and Nieminen R M 1986 *Phys. Rev.* B **34** 3820
[6] Rusz J, Biasini M and Czopnik A 2004 *Phys. Rev. Lett.* **93** 156405
[7] West R N 1992 *J. Phys. Chem. Solids* **53** 1669
[8] Sterne P A, Howell R H, Fluss M J, Kaiser J H, Kitazawa K and Kojima H 1993 *J. Phys. Chem. Solids* **54** 1231
[9] Berko S and Mills A P 1971 *J. Phys. Coll.* **32** C1 287
[10] Genoud P, Manuel A A, Walker E and Peter M 1991 *J. Phys.: Condens. Matter* **3** 4201
[11] Hanssen K E H and Mijnarends P E 1986 *Phys. Rev.* B **34** 5009
[12] Hanssen K E H, Mijnarends P E, Rabou P L M and Buschow K H J 1990 *Phys. Rev.* B **42** 1533
[13] Chiba T 1976 *J. Chem. Phys.* **64** 1182
Mijnarends P E and Singru R M 1974 *Appl. Phys.* **4** 303
[14] Mazin I I, Singh D J and Ambrosch-Draxl C 1999 *Phys. Rev.* B **59** 411
[15] Rusz J and Biasini M 2005 *Phys. Rev.* B **71** 233103
[16] Sorantin P and Schwarz K 1992 *Inorg. Chem.* **31** 567
[17] Kuneš J, Novák P, Oppeneer P M, König C, Fraune M, Rüdiger U, Güntherodt G and Ambrosch-Draxl C 2002 *Phys. Rev.* B **65** 165105
[18] Toropova A, Kotliar G, Savrasov S Y and Oudovenko V S 2005 *Phys. Rev.* B **71** 172403
[19] Hohenberg P and Kohn W 1964 *Phys. Rev.* **136** B864
Kohn W and Sham L J 1965 *Phys. Rev.* **140** A1133
[20] Perdew J P, Burke K and Ernzerhof M 1996 *Phys. Rev. Lett.* **77** 3865
[21] Zurmaev E Z, Moewes A, Butorin S M, Katsnelson M I, Finklstein L D, Nordgren J and Tedrow P M 2003 *Phys. Rev.* B **67** 155105
[22] Blaha P, Schwarz K, Madsen G K H, Kvasnicka D and Luitz J 2001 *WIEN2k* Vienna University of Technology (ISBN 3-9501031-1-2)
[23] Singh D, Pickett W E, von Stetten E C and Berko S 1990 *Phys. Rev.* B **42** R2696
[24] Biasini M and Rusz J 2006 *Phys. Rev.* B submitted
[25] Biasini M, Ferro G, Kontrym-Sznajd G and Czopnik A 2002 *Phys. Rev.* B **66** 075126